

Phase separation in colloidal suspensions induced by a solvent phase transition

Hartmut Löwen

Sektion Physik der Universität München, Theresienstrasse 37, D-80333 München, Germany

Received: 10 August 1994

Abstract. A colloidal suspension of macroparticles in a solvent is considered near a solvent first-order phase transition. The solvent phase transition is described by a Ginzburg-Landau model with a one-component order parameter which is coupled to the macroparticles coordinates. Wetting of the macroparticle surface by one of the two coexisting phases can induce phase separation of the colloidal particles. This phase separation is first explained by simple thermodynamic arguments and then confirmed by computer simulation of the Ginzburg-Landau model coupled to the macroparticles. Furthermore a topological diagnosis of the interface between the stable and metastable phase is given near phase separation and possible experimental consequences of the phase separation are discussed.

PACS: 82.70.Dd

1. Introduction

One of the most important questions in preparing colloidal suspensions concerns their stability against flocculation or coagulation due to the van-der-Waals attraction, for a review see Pusey [1]. There are two different mechanisms to stabilize a suspension: steric stabilization and charge stabilization. In the case of *steric stabilization* the colloidal particles are coated by blocked copolymer-brushes whose non-overlap condition guarantees repulsive forces between touching colloidal particles which overcome the van-der-Waals attraction. In *charged* colloidal suspensions, on the other hand, the thermal diffusivity of the counterion-layer around the charged colloidal surfaces leads to imperfect screening which also results in strong repulsive interparticle forces of electrostatic origin [2]. Flocculation and coagulation can be viewed as a special case of *phase separation* between the colloidal particles, one phase being the solvent alone and the other the cluster of sticking colloidal particles.

Now, even for stable colloidal suspensions, there may be phase separation into two different phases of the colloidal particles due to a different physical mechanism. The first possibility of such a phase separation was pointed out fourty years ago

by Asakura and Oosawa [3]. Due to a depletion zone of solvent molecules and added free polymer around the big colloidal particles there may be strong attractive forces for sterically-stabilized colloidal suspensions (see also Vrij [4]) which then may cause phase separation. Recent extensive computer simulations on a mixture of colloidal particles and added polymer chains with steric interactions confirm these attractions and a possible phase separation (see Meijer and Frenkel [5, 6]). Also the phase diagram of a colloid plus polymer system was experimentally completely investigated where a liquid-gas phase separation of the colloidal particles induced by the added polymer was found [7]. Another model to study effective attractions induced by depletion forces is a binary mixture of strongly asymmetric hard spheres. By a detailed study of liquid integral equations, Biben and Hansen [8, 9] found that the osmotic pressure by the small spheres exerted onto the big spheres yields phase separation of the big spheres if the diameter ratio is small. This kind of phase separation was also detected experimentally in strongly asymmetric bimodal suspensions of sterically stabilized colloidal spheres [10].

Second the long-ranged tail of the van-der-Waals attraction may cause a liquid-gas phase separation as theoretically discussed by Victor and Hansen [11, 12], for a survey see [1]. A third though still controversial mechanism for phase separation in charged suspensions are overscreening effects of the counterions due to strong counterion correlations see e. g. [13, 14]. However, to see this in a real suspension, the counterions have to be divalent and the bare charges of the colloidal particles have to be large.

The aim of this paper is to present a fourth mechanism for phase separation in colloidal suspensions which occurs if the solvent undergoes a first-order phase transition [15]. In the normal situation the solvent is in its fluid phase far away from any possible freezing or other first-order phase transition. If e.g. the temperature is lowered one may think of reaching the phase coexistence line of the solvent where another solvent phase may become stable forming some “islands” of the new phase in the sea of the old phase. It depends sensitively on the wetting properties of the colloidal particles whether the new phase or the old one covers the colloidal surfaces. In the first case the colloidal particles drag a cloud of the new phase

with themselves, in the opposite case the new phase occurs preferentially in voids between the colloidal particles. In this paper it is shown that a solvent first-order phase transition may drive a phase separation of the colloidal particles. The surface tension between the two solvent phases may dictate separation into one region where the colloidal particles are surrounded by one big cloud of the phase they prefer to be covered with and a second region occupied by the other solvent phase.

There are quite a number of possible realizations of the solvent phase transition. The first (and maybe the most natural) example is the freezing transition of a molecular fluid solvent into a regular solid. In the most common case of an aqueous suspension the corresponding freezing temperature is easily accessible experimentally. Inversely by enhancing the temperature also a first-order liquid-gas transition may happen. Another realization is a solvent mixture of two species A and B (e.g. water and alcohol) which can undergo a first order phase transition between an A -rich and a B -rich phase. If the solvent consists of a liquid crystal, a transition from the disordered to a nematic phase is conceivable and magnetic solvents may order from fluid-like into columnar phases. In the general theoretical framework all this different phase transitions can be described by an order parameter m distinguishing between the two phases. For the freezing, liquid-gas and the A -rich to B -rich transition, the order parameter m can be taken to be the relative density difference of the two coexisting phases. For a liquid-crystalline solvent it is the mean orientation and for magnetic solvents the mean magnetization of the two solvent phases.

As a final remark we state that also a solvent near its critical point represent a challenging question for theoreticians since the critical fluctuations may also induce exotic effective forces between the colloidal particles. Theoretical work has mainly focused to the much simpler geometry of a solvent between two parallel plates where attractive Casimir forces have been investigated, for a recent review see Krech [16]. The role of this Casimir forces between two spheres or even in an ensemble of randomly distributed spheres as in a colloidal suspension however is still unclear.

The paper is organized as follows: After an introduction and discussion of the Ginzburg-Landau model in chapter II, we describe analytical results for a situation far away from the phase transition by linearizing the equations in chapter III. Then, in chapter IV, simple thermodynamic arguments are used to explain the physical origin of the phase separation and to get different scenarios for it. The Ginzburg-Landau model is then completely solved by computer simulation. In chapter V we describe the numerical method and in chapter VI we present the results. We conclude with a comparison with experiments in chapter VII.

2. The model

We model the first-order phase transition of the solvent within the Ginzburg-Landau model [17] with a scalar order parameter field $m(\mathbf{r})$. m is chosen to be dimensionless. As already discussed before, m can have different meanings depending on

which solvent phase transition is considered. Hence the model is quite general and a different number of actual realizations are possible.

We are considering N colloidal particles in a given volume Ω with a particle number density $\rho = N/\Omega$, corresponding to a mean interparticle spacing of $a = \rho^{-1/3}$, and a fixed given temperature T . One configuration is characterized by the positions $\{\mathbf{R}_i, i = 1, \dots, N\}$ and the velocities $\{\dot{\mathbf{R}}_i, i = 1, \dots, N\}$ of the particles. Furthermore the particles interact via direct pairwise additive forces described by a direct interaction potential $V_{pp}(r)$. This interaction is repulsive for stabilized colloidal suspensions and may stem from pure excluded volume for sterically-stabilized suspensions or from incomplete counterion screening for charged colloidal suspensions. For the following we assume monodisperse particles and take a soft r^{-12} interaction for $V_{pp}(r)$:

$$V_{pp}(r) = k_B T G \left(\frac{\sigma}{r} \right)^{12} \quad (1)$$

where G is a prefactor of order 1 and σ a soft-sphere diameter.

The total Lagrangian \mathcal{L}_{tot} for the system consists of the macroparticle part and the free energy $\mathcal{F}([m(\mathbf{r})], \{\mathbf{R}_i\})$ of the order parameter field in the presence of the colloidal particles which depends parametrically on the macroparticle coordinates

$$\mathcal{L}_{\text{tot}} = \sum_{i=1}^N \frac{M}{2} \dot{\mathbf{R}}_i^2 - \sum_{i,j=1; i < j}^N V_{pp}(|\mathbf{R}_i - \mathbf{R}_j|) - \mathcal{F}([m(\mathbf{r})], \{\mathbf{R}_i\}) \quad (2)$$

where M is the macroparticle mass. This is a fictitious quantity since we are only interested in canonically averaged static quantities.

All important information on the solvent phase transition is contained in the free energy \mathcal{F} which is a *functional* of the order parameter field. Using the Ginzburg-Landau picture we model this functional as follows

$$\mathcal{F}([m(\mathbf{r})], \{\mathbf{R}_i\}) \equiv \mathcal{F}(\{\mathbf{R}_i\}) = \mathcal{F}_0[m(\mathbf{r})] + \mathcal{F}_{p0}([m(\mathbf{r})], \{\mathbf{R}_i\}) \quad (3)$$

Here $\mathcal{F}_0[m(\mathbf{r})]$ is the free energy functional for the decoupled system for which the following form is taken

$$\mathcal{F}_0[m(\mathbf{r})] = \int_{\Omega} d^3r \left[\frac{1}{2} f_0 \xi^2 (\nabla m(\mathbf{r}))^2 + f(m(\mathbf{r})) \right] + \frac{1}{2} \int_{\Omega} d^3r \int_{\Omega} d^3r' w(|\mathbf{r} - \mathbf{r}'|) m(\mathbf{r}) m(\mathbf{r}') \quad (4)$$

Let us discuss this functional in detail:

- i) For a spatially homogeneous order parameter field, $m(\mathbf{r}) \equiv m_0 \equiv \text{const}$, we have $\mathcal{F}_0[m(\mathbf{r})] = \Omega(f(m_0) + w_0 m_0^2/2)$ where w_0 is the zeroth moment of $w(r)$

$$w_0 = \int_{\Omega} d^3r w(r) \quad (5)$$

By a suitable subtraction in $w(r)$ it can be achieved without loss of generality that w_0 vanishes. Hence $f(m)$ contains the information about the solvent phase transition. Near

a solvent first-order phase transition, $f(m)$ possesses two minima of equal depth at m_1 and m_2 , corresponding to the two bulk order parameters of the coexisting phases. We model $f(m)$ by the usual m^4 -Ginzburg-Landau form

$$f(m) = f_0(m^4 - 2m^2 + 4\epsilon m) \quad (6)$$

where $f_0 > 0$ is a bulk free energy density scale and ϵ describes the mismatch with respect to coexistence. For $\epsilon = 0$, $f(m)$ exhibits two equal minima at $m_{\pm} = \pm 1$ (without loss of generality m can be scaled to be ± 1 in the two coexisting phases). For positive ϵ , the global minimum is at $m_- = 2 \cos(\phi/3 + 2\pi/3)/\sqrt{3}$ with $\phi = \arcsin(-3\sqrt{3}\epsilon/6)$ while it is at $m_+ = 2 \cos(\phi/3)/\sqrt{3}$ for negative ϵ .

- ii) The square-gradient term in (4) represents a free energy penalty for a inhomogeneous system and is practically nonzero only in the vicinity of an interface between the two coexisting phases. ξ a microscopic bulk correlation length governing the width of such an interface determining the surface tension.
- iii) The nonlocal interaction between the order parameter with the kernel $w(r)$ is a slight extension to the usual local Ginzburg-Landau model. It may be relevant to describe long-ranged interaction of the order parameter, see e.g. one example in the context of surface melting in [18].

The interaction between the order-parameter field and the colloidal particles is modelled by the following expression:

$$\mathcal{F}_{po}([m(\mathbf{r})], \{\mathbf{R}_i\}) = \int_{\Omega} d^3r \sum_{i=1}^N V_{po}(|\mathbf{R}_i - \mathbf{r}|) m(\mathbf{r}) \quad (7)$$

where $V_{po}(r)$ describes the interaction between the particles and the order parameter field. The action of $V_{po}(r)$ can be viewed to shift the coexistence parameter ϵ locally. If $V_{po}(r)$ is negative it will favour formation of the phase corresponding to the positive order parameter m_+ and vice versa. Normally $V_{po}(r)$ should contain a hard-core term due to the finite size of the particles. The occurrence of $V_{po}(r)$ may induce wetting [19] of the particle surface by the phase that is favoured by the particles. Even if this phase is not globally stable a mesoscopic portion of this phase may be formed at the particle surface. Since the particles are moving, the shape of this wetting layer changes in time and depends on the actual configuration $\{\mathbf{R}_i\}$ of the colloidal particles. Thus the problem is a wetting situation in a complicated geometry made up by the actual positions of the colloidal particles. It is the interaction of the wetting layer with the particles that may cause effective attractive interactions between the colloidal particles and may even drive a phase separation. This effective interaction is expected to have a strong many-body character and thus cannot be described well by an effective pair potential since the spatial region occupied by the wetting phase has a complicated shape and can also have a complicated topological structure containing holes, tubes etc. A typical situation is qualitatively shown in Fig. 1. The part of the wetting phase (grey zone) may be complicated and comprise one single, two or many particles

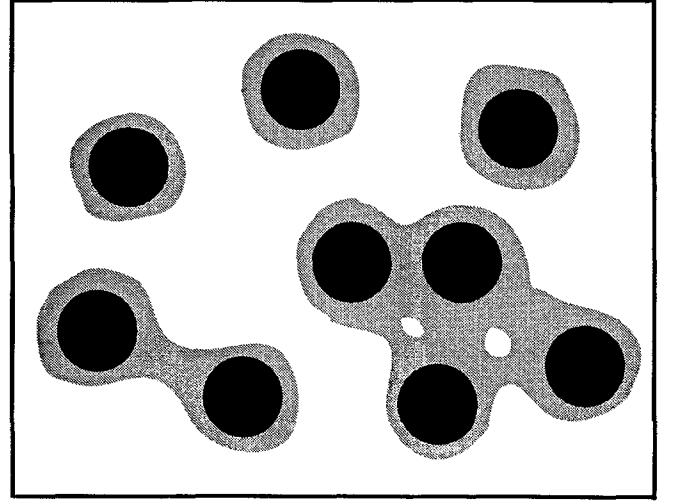


Fig. 1. Qualitative shape of the wetting phase (grey region) around the colloidal particles (black circles). This region can comprise several particles and can also have a complicated topology with holes etc

depending on the particle density and on the actual particle positions (black circles).

Mathematically the dynamic interface in the presence of the colloidal particles is obtained by solving Euler's equations of the Lagrangian \mathcal{L}_{tot} for the order parameter field

$$\frac{\delta \mathcal{F}([m(\mathbf{r})], \{\mathbf{R}_i\})}{\delta m(\mathbf{r})} = 0 \quad (8)$$

This yields the minimizing density field $m^{(0)}(\mathbf{r}, \{\mathbf{R}_i\})$ which depends parametrically on the particle coordinates. In performing the minimization there is a difference between a *conserved* or *nonconserved* order parameter. For a nonconserved order parameter the minimization is free, for a conserved one it is subjected to the constraint

$$\frac{1}{\Omega} \int_{\Omega} d^3r m(\mathbf{r}) = \bar{m} \quad (9)$$

where \bar{m} is the mean value of the order parameter which is an additional input variable. This constraint can be easily incorporated into the Lagrangian \mathcal{L}_{tot} by using a Lagrange multiplier. Finally Euler's equations for the particle coordinates read

$$M \ddot{\mathbf{R}}_i = -\nabla_{\mathbf{R}_i} \sum_{j:j \neq i}^N V_{pp}(|\mathbf{R}_j - \mathbf{R}_i|) + \mathbf{F}_i^p \quad (10)$$

In addition to the direct forces stemming from $V_{pp}(r)$ there are effective pseudo-forces \mathbf{F}_i^p on the macroparticles induced by the solvent order parameter field

$$\mathbf{F}_i^p = - \int_{\Omega} d^3r m^{(0)}(\mathbf{r}, \{\mathbf{R}_j\}) \nabla_{\mathbf{R}_i} V_{po}(|\mathbf{r} - \mathbf{R}_i|) \quad (11)$$

These pseudo-forces clearly exhibit a *many-body character*. It is only in the case of a quadratic functional that these forces become pairwise. This is discussed in detail in the next section. As a final remark we mention that Frink and van Swol

have recently also considered a similar approach to model the nature of the solvent [20]. Their calculation, however, does not include a first order phase transition of the solvent.

3. Quadratic expansion of the functional

Far away from coexistence the solvent practically is in one bulk phase described by a nearly constant order parameter field $m(\mathbf{r}) = m_0$ where m_0 is the minimum of the free energy density $f(m)$. If only small deviations from m_0 are considered, it is justified to expand the nonlinear free energy density $f(m)$ up to second order

$$f(m) \approx f(m_0) + \frac{1}{2} f_2 (m - m_0)^2 \quad (12)$$

where $f(m_0)$ is an additive constant which can be set to zero without loss of generality and $f_2 = d^2 f(m_0)/dm^2 > 0$. If $f(m)$ is replaced by its quadratic expansion (12), the free energy functional is completely quadratic and the minimization equation is linear in $m(\mathbf{r})$. Consequently, the minimization of the functional with respect to the order parameter field can be done *analytically* by Fourier transformation. The resulting minimizing order parameter field $m^{(0)}(\mathbf{r}, \{\mathbf{R}_i\})$ in the field of N macroparticles then is a linear superposition of orbitals $\hat{m}(\mathbf{r})$:

$$m^{(0)}(\mathbf{r}, \{\mathbf{R}_i\}) = m_0 + \mu + \sum_{i=1}^N \hat{m}(|\mathbf{r} - \mathbf{R}_i|) \quad (13)$$

The orbitals are explicitly given by

$$\hat{m}(\mathbf{r}) = - \int d^3 k \times \exp(-i\mathbf{k} \cdot \mathbf{r}) \frac{\tilde{V}_{po}(k)}{f_2 + f_0(\xi k)^2 + (2\pi)^3 \tilde{w}(k)} \quad (14)$$

where $\tilde{V}_{po}(k)$ is the Fourier transform of the particle-order-parameter interaction

$$\tilde{V}_{po}(k) = \frac{1}{(2\pi)^3} \int d^3 r \exp(i\mathbf{k} \cdot \mathbf{r}) V_{po}(r) \quad (15)$$

Likewise $\tilde{w}(k)$ is the Fourier transform of $w(r)$. Furthermore, in (13), μ is a Lagrange multiplier which guarantees the given averaged value \bar{m} of the order parameter field if it is conserved. For a non-conserved order parameter μ is zero.

The *linear* superposition of orbitals finally yields to an effective *pairwise* interaction between the macroparticles induced by the solvent order parameter. The effective interaction can be described by the spherical-symmetric pair-potential

$$V_{\text{eff}}(r) = - (2\pi)^3 \int d^3 k \times \exp(-i\mathbf{k} \cdot \mathbf{r}) \frac{\tilde{V}_{po}^2(k)}{f_2 + f_0(\xi k)^2 + (2\pi)^3 \tilde{w}(k)} \quad (16)$$

Several remarks are in order: First, if the sign of $V_{po}(r)$ is reversed the effective interaction does not change. If $w(r) = 0$ and $V_{po}(r)$ has a fixed sign, $V_{po}(r) \geq 0$ or $V_{po}(r) \leq 0$, one

can easily show that $V_{\text{eff}}(r) \leq 0$. This implies that the effective forces between the colloidal particles induced by the solvent order parameter are always attractive in this case. If this attraction is strong enough it may drive liquid-gas phase separation. Second, if the solvent is far away from any phase transition, $V_{po}(r)$ is short-ranged and small [21], so this effective attraction can completely be neglected. Third, the effective interaction does not depend on whether the order parameter is conserved or not.

More explicit results for $\hat{m}(\mathbf{r})$ and $V_{\text{eff}}(r)$ can be obtained if $V_{po}(r)$ and $w(r)$ are explicitly specified. One simple example is a contact interaction

$$V_{po}(r) = V_0 \delta(r) \quad (17)$$

which may be repulsive or attractive depending on the sign of V_0 together with a vanishing non-local interaction, $w(r) = 0$. In this case one obtains a Yukawa form for the order parameter orbital

$$\hat{m}(\mathbf{r}) = - \frac{V_0}{4\pi f_0 \xi^2 r} \exp\left(-\sqrt{\frac{f_2}{f_0}} r/\xi\right) \quad (18)$$

and an effective Yukawa attraction between the macroparticles

$$V_{\text{eff}}(r) = - \frac{V_0^2}{4\pi f_0 \xi^2 r} \exp\left(-\sqrt{\frac{f_2}{f_0}} r/\xi\right) \quad (19)$$

irrespective of the sign of V_0 . These results for $\hat{m}(\mathbf{r})$ and $V_{\text{eff}}(r)$ are visualized in Figs. 2 and 3 where also two other cases for $V_{po}(r)$ are displayed ($w(r)$ is always chosen to be zero): a square well potential

$$V_{po}(r) = V_0 \Theta(R - r) \quad (20)$$

$\Theta(x)$ denoting the unit step function, and a potential with alternating sign consisting of two δ -peaks, an attractive one at the origin and a repulsive one at a certain distance R , i.e.

$$V_{po}(r) = V_0(\delta(r) - c \delta(R - r)) \quad (21)$$

with $c > 0$. While the square-well potential which is more realistic than the contact interaction qualitatively shows the same orbital and effective pair-potential as the exactly soluble contact interaction (17), an oscillating form of $V_{po}(r)$ may also induce oscillations in $V_{\text{eff}}(r)$.

It is easily shown that an effective pair-potential is *equivalent* to a quadratic free energy functional. Near a first order phase transition of the solvent, however, $f(m)$ is highly nonlinear with two minima representing the two coexisting phases. It is thus expected that there are massive corrections to the approximate pair-potential description given by (16). These corrections intrinsically contain many-body forces between the particles induced by the particle-order-parameter interaction. Since one cannot solve the minimizing equation for the order-parameter profile analytically in this case, one is forced to perform a numerical simulation of the particle-order-parameter interaction. This is described in detail in Sect. 5.

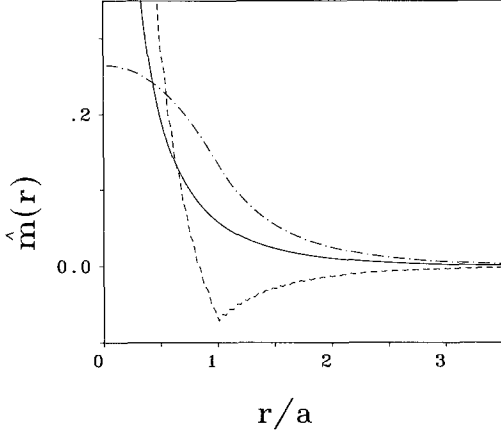


Fig. 2. Order parameter orbitals $\hat{m}(r)$ versus r in the quadratic approximation for three different particle-order-parameter interactions $V_{po}(r)$. i) contact interaction (solid line): $V_{po}(r) = -V_0\delta(r)$; ii) square well interaction (dot-dashed line): $V_{po}(r) = -V_0\Theta(a-r)/a^3$; iii) “oscillating interaction” (dotted line): $V_{po}(r) = -V_0(5\delta(r) - \frac{1}{2}\frac{V_0}{a^2}\delta(r-a))$. Here, $V_0 > 0$ sets the energy and a the length scale. The other model parameters are $\xi = \sqrt{V_0/a f_0}$, $f_0 = V_0/a^3$

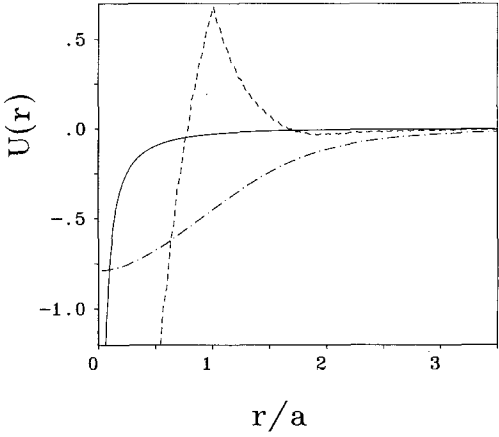


Fig. 3. Same as Fig. 2 but now for the effective interaction potential $V_{\text{eff}}(r) \equiv U(r)$ between two macroparticles which is measured in units of V_0

4. Simplified picture of the phase separation

In order to get a qualitative insight into the physical mechanism driving a colloid phase separation we first give a *simplified picture* using simple thermodynamic arguments. In considering a situation with an order parameter field describing a situation near coexistence of a phase A with a phase B we adopt the following approximations:

- i) The order parameter field is taken to be either $m_A \equiv 1$ or $m_B \equiv -1$ with an infinitely sharp interface between the A and B region. This means that microscopic details of the order parameter field are neglected.
- ii) The complicated structure of the AB -interface as sketched in Fig. 1 is either completely neglected or approximated by nonoverlapping spheres around the colloidal particles. This is the strongest assumption we make.

- iii) We neglect long-ranged order parameter interactions, i.e. $w(r) \equiv 0$. This is not a severe approximation.

Without loss of generality we assume that A is the metastable phase and that A wets the colloidal spheres. Consider the thermodynamic stability of two different situations a) and b). In the first case a) the colloidal spheres are in a fluid phase and covered by a mesoscopic spherical drop of the metastable solvent phase A belonging to an order parameter $m_A \equiv 1$ while the rest of space is covered by the stable phase B characterized by an order parameter $m_B \equiv -1$. In the second situation b) there are only two simple-connected regions of space for the A and B phase corresponding to a volume of Ω_A and Ω_B such that the total volume Ω equals $\Omega_A + \Omega_B$. In both regions the colloidal particles are in a fluid phase. However their density is different in both regions, in general: it is $\rho_A = N_A/\Omega_A$ in the A -region and $\rho_B = N_B/\Omega_B$ in the B -region such that $\rho = N/\Omega = (N_A + N_B)/(\Omega_A + \Omega_B)$. There are two extreme cases of b) which we call c) and d): In situation c) there is no region with phase A ($\Omega_A = 0$) while in d) phase B is absent ($\Omega_B = 0$). All situations a) - d) are sketched in Fig. 4.

4.1. Conserved order parameter

We first assume that the order parameter is *conserved* with a given mean value \bar{m} , $-1 \equiv m_B < \bar{m} < m_A \equiv 1$. This implies

$$\bar{m} = m_A \frac{\Omega_A}{\Omega} + m_B \left(1 - \frac{\Omega_A}{\Omega}\right) \quad (22)$$

Hence Ω_A is fixed by $\Omega_A = \Omega(\bar{m} + 1)/2$. In situation a), the total free energy of the non-phase-separated system is approximately given by

$$F_1(\Omega_A) = 8f_0\epsilon\Omega_A + \Omega f_p(\rho, T) + N\gamma 4\pi R^2(\Omega_A) + N f_1^c(\Omega_A) \quad (23)$$

Let us explain the different terms in detail: First $8f_0\epsilon\Omega_A$ is the free energy cost to create a volume Ω_A of phase A where $\epsilon > 0$ measures the distance to coexistence of A and B . Furthermore $f_p(\rho, T)$ is the bulk free energy per unit volume of a fluid interacting solely via the pair potential $V_{pp}(r)$. For $V_{pp}(r) = k_B T G(\sigma/r)^{12}$, all static quantities only depend on the so-called coupling parameter

$$\Gamma = \rho\sigma^3(G/4)^{1/4} \quad (24)$$

Hansen [22] has given an empirical fit for $f_p(\rho, T)$ based on Monte Carlo data (see also Pastore and Waisman [23]):

$$f_p(\rho, T)/(k_B T \rho) = \ln(\rho\sigma^3) - 1 + 3.629\Gamma + 3.632\Gamma^2 + 3.4975\Gamma^3 + 2.86475\Gamma^4 + 0.217619\Gamma^{10} \quad (25)$$

which is valid for the whole fluid range up to freezing occurring at $\Gamma = 0.814$ [22]. Furthermore in Eq. (23), γ is the surface tension of the AB interface which can be exactly calculated at coexistence ($\epsilon = 0$) for a *planar* AB -interface resulting in

$$\gamma = \frac{4}{3}\sqrt{2}f_0\xi \quad (26)$$

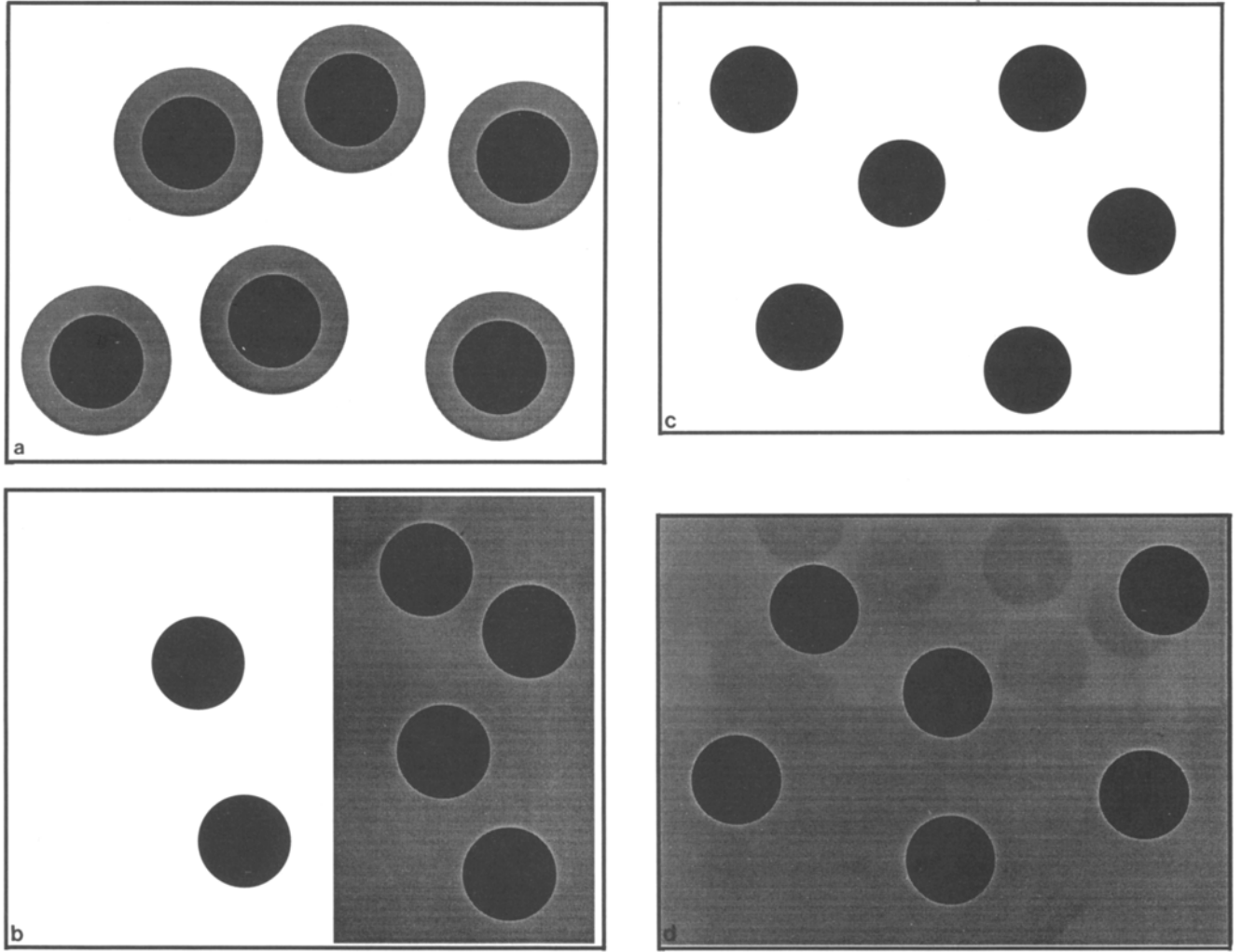


Fig. 4a–d. Sketch of the four situations considered in Sect. 4: **a** each colloidal sphere is surrounded by a spherical drop of the metastable phase A with radius R ; **b** one region of space with volume Ω_A is occupied by phase A and the colloidal particles having a density ρ_A , the other part is occupied by phase B with a different colloid density ρ_B ; **c** all colloidal spheres are contained in one large region of the stable phase B ; **d** all colloidal spheres are contained in one large region of the metastable phase A . Situations **c** and **d** are two extreme limits of **b**

Moreover R is the radius of the phase A droplets

$$R(\Omega_A) = \left(\frac{3}{4\pi\rho} \frac{\Omega_A}{\Omega} \right)^{1/3} \quad (27)$$

Finally the energy gain in wetting the colloidal surfaces by phase A is accounted for by the term $N f_1^c(\Omega_A)$ where

$$f_1^c(\Omega_A) = 4\pi m_A \int_0^{R(\Omega_A)} dr r^2 V_{po}(r) + 4\pi m_B \int_{R(\Omega_A)}^{\infty} dr r^2 V_{po}(r) \quad (28)$$

Note that for our situation $f_1^c(\Omega_A)$ is negative. We state two comments on the droplet situation a): First, it only makes sense for $\Omega_A/\Omega < \pi\sqrt{2}/6 = 0.74048$ which is the volume fraction of dense-packed spheres. Second, the total surface tension is overestimated since the spheres do not fuse which would result in a drastic reduction of the free energy.

In the second situation b) similar arguments lead directly to the following expression for the total free energy

$$F_2(\Omega_A, N_A) = 8f_0\epsilon\Omega_A + \Omega_A f_p \left(\frac{N_A}{\Omega_A}, T \right) + (\Omega - \Omega_A) f_p \left(\frac{N - N_A}{\Omega - \Omega_A}, T \right) + N_A f_2^c - (N - N_A) f_2^c \quad (29)$$

with

$$f_2^c = 4\pi \int_0^{\infty} dr r^2 V_{po}(r) \quad (30)$$

since the colloidal particles are now completely surrounded by one big volume either of phase A or B . The free energies belonging to the special cases c) resp. d) are easily obtained by setting $\Omega_A = 0$ resp. $\Omega_A = \Omega$ in (29). The physical realized value $N_A^{(0)}$ of N_A corresponds to the minimum of $F_2(\Omega_A, N_A)$ with respect to N_A within the bounds $0 \leq N_A \leq N$. Clearly this minimum is a function of Ω_A , i.e. $N_A^{(0)} = N_A^{(0)}(\Omega_A)$.

Phase separation occurs if the free energy of situation b) is lower than that of situation a)

$$F_2(\Omega_A, N_A^{(0)}) < F_1(\Omega_A) \quad (31)$$

and if the the partial densities differ $\rho_A = N_A/\Omega_A \neq N_B/\Omega_B = \rho_B$.

4.2. Non-conserved order parameter

For a *non-conserved* order parameter the expression for the free energies $F_1(\Omega_A)$ and $F_2(\Omega_A, N_A)$ are the same but Ω_A is not fixed but adapts itself such that it minimizes $F_1(\Omega_A)$ resp. $F_2(\Omega_A, N_A^{(0)}(\Omega_A))$ for fixed given ρ and T . Let $\Omega_A^{(1)}$ be the minimizing volume of $F_1(\Omega_A)$ and $\Omega_A^{(2)}$ be that of $F_2(\Omega_A, N_A^{(0)}(\Omega_A))$.

Now phase separation occurs if

$$F_2(\Omega_A^{(2)}, N_A^{(0)}) < F_1(\Omega_A^{(1)}) \quad (32)$$

and if the minimizing volume $\Omega_A^{(2)}$ is different from 0 and Ω and if $\rho_A \neq \rho_B$. In general, $\Omega_A^{(1)} \neq \Omega_A^{(2)}$ which implies that the condition (31) differs from (32).

Using the condition (32), the region of phase separation was investigated for different surface tensions γ and varying ϵ . In an experiment, typically all material parameters are fixed and one basically varies the distance to coexistence ϵ by changing the temperature for instance. Therefore we have investigated the region of phase separation using the condition (32) for varying ϵ including also different surface tensions γ . One result is shown in Fig. 5. One sees that all four different situations a) - d) do occur. Experimental paths are parallel to the ϵ -axis. Obviously far away from coexistence ($\epsilon \rightarrow \infty$) situation c) is stable while at coexistence ($\epsilon = 0$) all space is filled up with the formerly metastable phase A. In between there is a phase separation line and there are different scenarios which one may encounter experimentally. If one reduces ϵ for low γ there is first of all a transition from c) to a) where one observes droplets. Then phase separation occurs in crossing from a) to d). For large γ the intermediate droplet situation a) is not realized. In between there is an interesting possibility for phase separation from c) to b) and then a re-transition into a one-phase region a) and again a phase separation towards b). Of course in situation b), $\rho_A > \rho$ and $\rho_B < \rho$.

For a conserved order parameter the situation is of course more difficult since also \bar{m} has to be prescribed.

In the following we shall abandon these simple considerations but solve the full Ginzburg-Landau model by computer simulation. We shall see that the phase separation found there is consistent with the phenomenological arguments of this section. This strongly supports the view that the full solution does not destroy qualitative aspects of the phase separation line but may give rise to a significant shift of the phase separation line with respect to the simplified results of this section. It is also expected that a non-vanishing kernel $w(r)$ only shifts the phase separation line but does not change the scenario qualitatively.

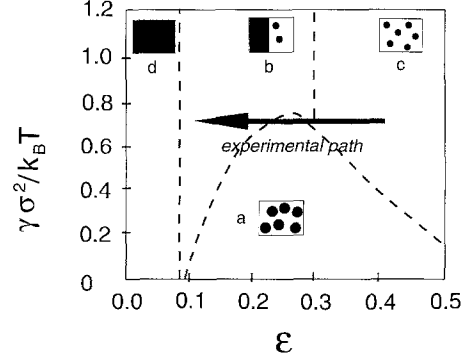


Fig. 5. Stability of the four different situations **a-d** in the ϵ - γ -plane as predicted by the simple considerations of Sect. 4. γ is given in units of $k_B T/\sigma^2$. The dashed lines separate the different situations **a-d**. An experimental path ($\gamma = \text{const}$) is also shown by the arrow. We have taken a non-conserved order parameter with an interaction $V_{pp}(r) = -30k_B T \sigma^{-3} \exp(-11.1(r/\sigma)^2)$. The remaining parameters are $G = 10$, $f_0 = 2k_B T/\sigma^3$, $\rho = 0.382\sigma^{-3}$

5. Computer simulation of the phase separation

A full computer simulation of the Ginzburg-Landau model can be achieved by using a classical version of the Car-Parrinello algorithm [24] which was already applied to charged colloidal suspensions [25, 26] where the counterionic density field was explicitly taken into account, for another application see [27]. Here we proceed in a similar fashion. We take $N=108$ colloidal particles in a cubic box with periodic boundary conditions and parametrize the order parameter field by its Fourier expansion

$$m(\mathbf{r}) = \sum_{\mathbf{G}} m_{\mathbf{G}} \exp(i\mathbf{G} \cdot \mathbf{r}) \quad (33)$$

where the sum is over all reciprocal lattice vectors \mathbf{G} of the cubic box. In practice this sum has to be cut off; we include of about 262000 different reciprocal lattice vectors corresponding to an order parameter field in real space on a 64^3 cubic grid. Following Car and Parrinello, we add a fake kinetic energy term

$$K_f = \frac{1}{2} \sum_{\mathbf{G}} g_{\mathbf{G}} \left\{ \frac{dm_{\mathbf{G}}}{dt} \right\}^2 \quad (34)$$

to the total Lagrangian \mathcal{L}_{tot} , see Eq. (2). From a preconditioning method proposed in [27], we examine the exactly soluble case where $f(m)$ is a parabola and determine the fake mass to be $g_{\mathbf{G}} = g_0(1 + (\xi G)^2/4)$ where g_0 is chosen sufficiently small such that the fake kinetic energy K_f remains small during the simulation. The starting configuration of the colloidal particles was gained from an ordinary Molecular Dynamics simulation for a system with $V_{pp}(r)$ as the only interaction. The minimum of the order parameter field was obtained by a simulated annealing method [26]. The Euler equations of motion were solved for the colloid positions (see (gradient))

and for the fictitious coordinates $\{m_G\}$ using a finite time step method. After a long equilibration period statistics were gathered for the colloid+order-parameter-field system. One time step consumed of about 0.5 seconds on a Cray YMP. One run took of about 10000-20000 time steps. By watching the positions of the colloids one can check whether they are in a phase-separated state or in one single fluid phase.

We have used the following form for $V_{po}(r)$ in our calculations:

$$V_{po}(r) = Ek_B T \sigma^{-3} \exp(-(r/\lambda)^2)$$

with a dimensionless amplitude E usually taken to be negative and a range λ . In order to keep the model simple, we furthermore assume a vanishing long-ranged order parameter interaction although its incorporation would be straightforward in the Car-Parrinello method. We have performed four runs A, B, C and D the parameters of which are summarized in Table 1. The order parameter was always taken to be conserved. A non-conserved order parameter field can be treated in the same fashion.

Table 1. Parameters of the four different runs A, B, C and D. Given are the soft-sphere interaction amplitude G , the order parameter correlation length ξ , the free energy density scale f_0 , the distance ϵ from coexistence, the mean order parameter \bar{m} . The coupling potential $V_{po}(r)$ is taken to be $V_{po}(r) = Ek_B T \sigma^3 \exp(-(r/\lambda)^2)$ where the amplitude E the the range λ are also given. The density of the colloidal particles is fixed to be $\rho = 0.382\sigma^{-3}$. The order parameter is assumed to be conserved

run	G	ξ/σ	$f_0\sigma^3/k_B T \epsilon$	\bar{m}	E	λ/σ
A	4	0.224	0.4	0	-0.05	0.5
B	0.1	0.2	2.5	0.1	-1	0.6
C	0.1	0.245	5.	0.1	-2	0.75
D	4	0.05	2	0.1	-0.5	-2

6. Results

6.1. Pair correlation function

One of the key quantities characterizing static correlations in the fluid state is the pair correlation function $g(r)$ which is defined as

$$g(r) = \frac{1}{\rho N} \sum_{i,j=1; i \neq j}^N \langle \delta(\mathbf{r} - (\mathbf{R}_i - \mathbf{R}_j)) \rangle \quad (35)$$

where $\langle \dots \rangle$ denotes a canonical average. Results for $g(r)$ for the four different runs A-D are shown in Figs. 6 and 7. Here also the results for a pure soft sphere system ($V_{po}(r) \equiv 0$) are shown. In a non-phase-separated situation, the height of the first maximum in $g(r)$ is a measure for the strength of the interparticle interaction provided the particle density ρ and the

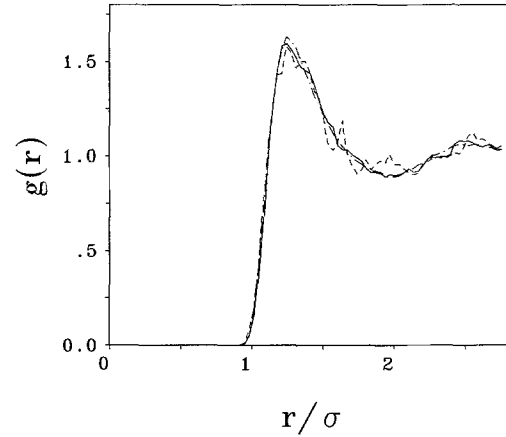


Fig. 6. Pair correlation function $g(r)$ versus r/σ for run A (solid line) and run D (dashed line). For comparison also the result for the pure soft-sphere interaction is also given (dot-dashed line). The dashed curve has a large statistical error. The three curves practically coincide

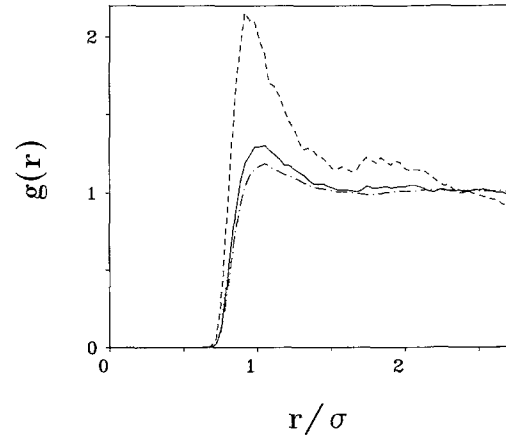


Fig. 7. Pair correlation function $g(r)$ versus r/σ for run B (solid line) and run C (dashed line). For comparison also the result for the pure soft-sphere interaction is also given (dot-dashed line). The results indicate a region with a higher density indicating colloid phase separation

temperature T are fixed. On the other hand, the position of the first maximum is a measure for the mean interparticle distance.

For run A (Fig. 6), $V_{po}(r)$ is small and hence $g(r)$ practically coincides with that of the pure soft sphere case. This implies that the pseudo-forces are negligibly small compared to the direct forces stemming from the soft-sphere interaction. In run B (Fig. 7), the positions of the first maximum shifts a bit to a smaller values as compared to the soft-sphere reference case. This indicates that in a certain region of space there is a particle density that is higher than ρ . Correspondingly the height has increased also pointing out that in the denser space the correlations are stronger. This trend is much more pronounced in run C (Fig. 7) where there is a significant shift in the position to smaller values and also a height that is much larger than in the soft-sphere case. We thus may tentatively classify runs B and C as being phase-separated. Finally the $g(r)$ in run D (Fig. 6) is within the large statistical error also

identical to the soft-sphere result indicating that the situation is not phase-separated.

6.2. Typical configurations

Whether there is phase separation or not is more directly seen if one considers configurations of the colloidal particles and the interface between the metastable phase A and the stable phase B . In Fig. 8, a slab with size $L \times L \times L/3$ is considered comprising the xy plane of the cubic simulational box and a third of the length in z -direction. Here L is the box length. The projection of the colloid positions onto the xy -plane is denoted by circles. To visualize the location of the interface we have averaged the order parameter field along the z direction for each real space grid point of the xy -plane. If it is negative belonging to the region of phase A , it is denoted by a black point. In the opposite case, it is not marked. Hence the white region corresponds to phase B and dotted region to phase A . For runs A and B (Figs. 8a, b) there is only one single-connected region of phase A . The density ρ_A in this region is discussed in 6.4. In run C, all particles are surrounded by one big region of phase A while in run D (Fig. 8d) the AB interface has a complicated structure and depends heavily on the configuration of the colloidal particles. Hence, it is clear that run C is in a phase-separated situation and D is not phase separated.

6.3. Fit of the effective many-body forces by an optimal pair-potential

During the simulation we stored the effective pseudo-forces $\{\mathbf{F}_i^p\}$ and the corresponding positions $\{\mathbf{R}_i\}$ of the colloidal particles. These effective forces exhibit a many-body character. It is interesting to check whether they can be fitted by an effective pair-potential $V(r)$ by minimizing the expression

$$\sum_{i=1}^N \left(\mathbf{F}_i^p + \sum_{k=1; k \neq i}^N \frac{\partial V(r)}{\partial r} \frac{\mathbf{r}}{r} \Big|_{r=|\mathbf{R}_i - \mathbf{R}_k} \right)^2 \quad (36)$$

In the context of charged colloidal suspensions such an optimal effective pair-potential can be found which then represents a simple but reasonable approximation for the total effective interparticle forces [28]. In our case the pseudo-forces could not be well fitted by a pair-potential. On the level of the force the deviations were always of the order of 30%! This indicates that the interaction has an important non-trivial many-body character where the whole cluster with many colloidal particles surrounded by the metastable phase A contributes to the pseudoforces.

6.4. Partial densities: comparison with the simplified picture

For runs A, B and C simulation results for the partial densities ρ_A and ρ_B of the colloidal particles in the A resp. B region are summarized in Table 2. Run A corresponds to situation b) with $\rho_A = \rho_B = \rho$. Hence, in accordance with our previous

findings, there is no phase separation for run A. In run B, however, ρ_A differs from ρ_B . Consequently, this is a phase-separated situation b). In run C, one extreme limit of situation b), namely the special case $\rho_B = 0$ is realized, we can speak of *complete phase separation*. Finally for run D, the partial densities are not well-defined.

The simplified picture of Sect. 4 predicts the stability of situation b) against situation a) for the parameter combinations of *all* four runs A-D. Consequently, the situation of run D which is a) rather than b) is not well-described. This is of course due to the approximation of nonoverlapping spheres: the surface tension is strongly overestimated since the nonoverlapping spheres have a large surface that is drastically reduced in reality, see again Fig. 8d. For runs A, B and C the results of the simplified picture are very satisfactory. It reproduces the homogeneous situation of run A and the complete phase separation of run C. In run B the non-trivial partial densities are reproduced with an accuracy of less than 5%. Hence the simple picture is capable to predict phase separation lines in situation which do not involve situation a).

6.5. Topological diagnosis of the interface at phase separation

One natural topological quantity is the number of clusters per particle $n_c = \langle N_c \rangle / N$ of the metastable phase A where $\langle N_c \rangle$ is the canonical average of the number of connected A -clusters. (An A -cluster is a single-connected region of space containing a negative order parameter field.) In situations b), c), d) of the simplified picture, n_c vanishes since there is only one big cluster of phase A . In situation a), on the other hand, we get $n_c = 1$. This, however, is an upper bound since in a realistic situation the spheres are overlapping and form common clusters such that $n_c < 1$ on average.

We have calculated n_c from our simulational data using the Hoshen-Kopelman algorithm [29]. The results for n_c in the different runs A-D are summarized in Table 2. In run D, we have $n_c = 0.40$ while in all other runs n_c vanishes. One may expect that the route towards phase separation from a situation a) occurs in such a way that n_c decreases continuously and then jumps discontinuously from a critical value $n_c^{(c)} > 0$ to zero. The finite value of $n_c^{(c)}$ corresponds to a percolation threshold, see [30].

Table 2. Partial densities ρ_A and ρ_B resulting from the computer simulation for runs A, B, C and D. For comparison also the results for the partial densities from the simplified picture of Sect. 4 are given ($\rho_A^{(s)}$ resp. $\rho_B^{(s)}$). For run D, ρ_A and ρ_B are not defined. However, the simplified picture yields the stability of situation b) rather than the correct situation a). Also given is the averaged number n_c of order parameter clusters per particle

run	ρ_A / ρ	ρ_B / ρ	$\rho_A^{(s)} / \rho$	$\rho_B^{(s)} / \rho$	n_c
A	1.00	1.00	1.00	1.00	0
B	1.39	0.61	1.42	0.58	0
C	2.00	0.00	2.00	0.00	0
D	-	-	1.19	0.94	0.40

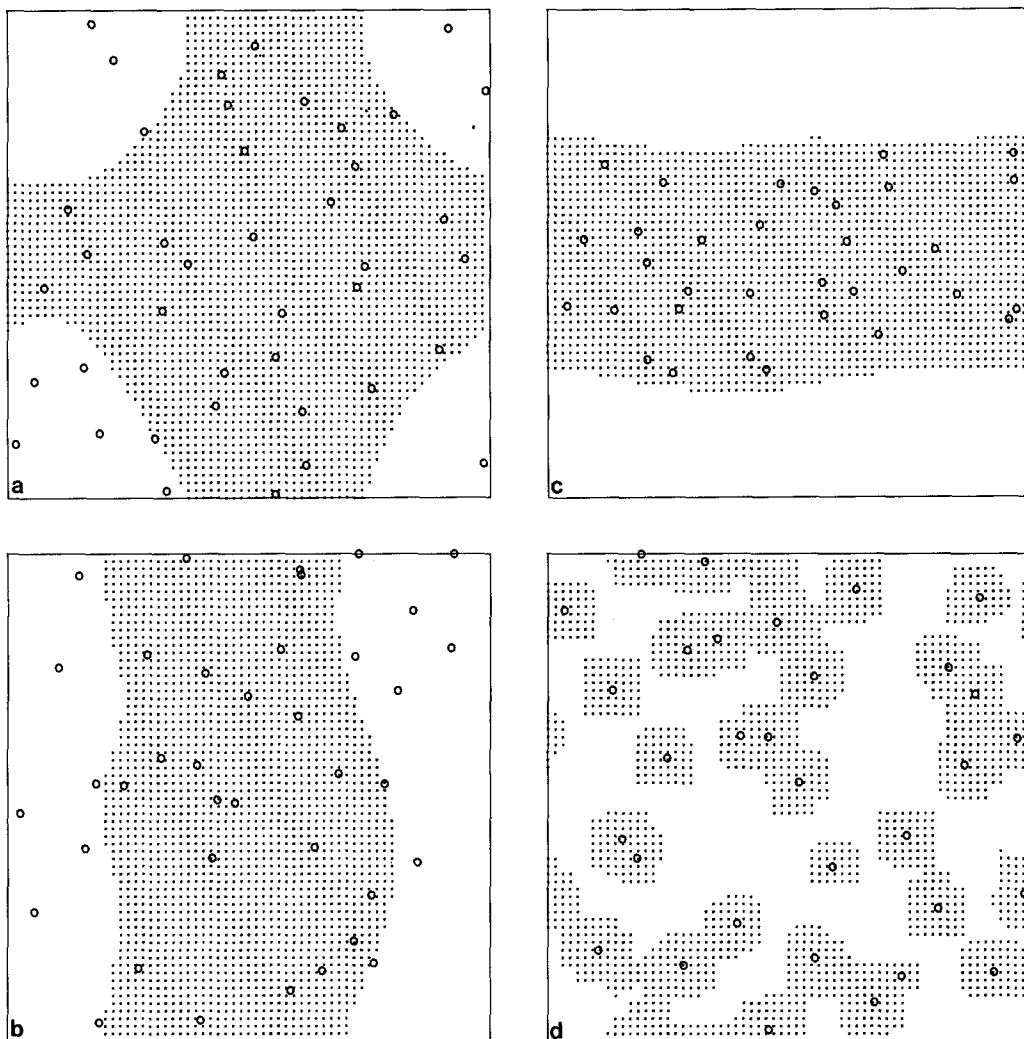


Fig. 8a-d. Typical configurations of the colloidal particles and the AB interface. The spheres denote the positions of the colloidal particles projected to the xy -plane of the cubic simulational box having a length L . Only a slab is considered, i.e. only positions with a z -component between 0 and $L/3$ are shown. The resolution of the dark pixels exactly corresponds to the finite real-space grid in the xy -plane used in the simulations. There is a dark pixel if the z -average of the order parameter field over the slab is positive which means that there is more of the metastable phase A . A white region indicates the opposite, namely that the z -average of the order parameter field is negative. **a** For run A. **b** For run B. **c** For run C. **d** For run D

One may further speculate that the Euler characteristic of the AB -interface may reveal further interesting diagnosis of the phase separation. The relation of the Euler characteristic to percolation problems has been clarified by Mecke and Wagner [31]. It has also recently been applied to characterize the structure of membranes and microemulsions [32].

7. Conclusions

In conclusion, we have discussed a colloid phase separation driven by a first-order phase transition of the solvent. The metastable phase wets the colloidal surfaces forming clusters of this solvent phase around the colloidal particles. The system can reduce its free energy by separating into two different regions: one is filled with the metastable phase and contains colloidal particles with a higher number density than the

global average, the other region with the stable solvent phase contains only few colloidal particles. With a simple thermodynamic model, qualitative diagrams with different routes towards phase separation have been discussed. Based on a Ginzburg-Landau model, computer simulations have also been performed resulting e.g. in a topological diagnosis of the interface between the two solvent phases.

One challenging problem is to calculate a complete phase separation diagram with computer simulation and use realistic material parameters to describe an experiment. Since this requires a multitude of different runs, it is a difficult task. More modestly, one can look whether there are experiments which exhibit at least qualitatively the scenario of phase separation proposed in this paper. A series of interesting experiments have been performed by Beysens and coworkers on colloidal silica spheres with a solvent mixture consisting of water and lutidine [33, 34]. In the vicinity of the lower consolute point of

the solvent mixture the colloidal spheres aggregate since they cover themselves with a lutidine-rich layer. Hence it appears that this aggregation is exactly the phase separation discussed in our paper. Also the effect of added salt was studied and it was found that the flocculation disappeared when salt was added [35]. Within our theoretical approach this can be understood qualitatively as a change in the interaction between the colloidal particles and the order parameter field due to the presence of salt at the colloidal surfaces. More recently experiments on silica colloids in reentrant liquid mixtures of 3-methylpyridine plus water plus heavy water exhibit a similar flocculation near the solvent phase transition [36].

Recently Palberg [37] reported another interesting phase separation in highly salted aqueous colloidal suspensions near the ice freezing point. He observed that there are mesoscopic regions of ice containing no colloidal spheres. So fluid water wets the colloidal surfaces rather than ice. The phase separation mechanism can thus effectively be exploited to concentrate suspensions by cooling them down and removing the mesoscopic icy parts.

I thank Herbert Wagner, Gerhard Gompper, Thomas Palberg and Jean-Louis Barrat for helpful discussions. This paper is dedicated to Herbert Wagner on the occasion of his 60th birthday.

References

1. For recent reviews, see P. N. Pusey, in "Liquids, Freezing and the Glass Transition", edited by J. P. Hansen, D. Levesque and J. Zinn-Justin, North Holland, Amsterdam, (1991).
2. E. J. W. Verwey and J. T. G. Overbeek, "Theory of the Stability of Lyophobic Colloids" Elsevier, Amsterdam, (1948).
3. S. Asakura, F. Oosawa, J. Chem. Phys. **22**, 1255 (1954).
4. A. Vrij, Pure and Applied Chem. **48**, 471 (1976).
5. E. J. Meijer, D. Frenkel, Phys. Rev. Lett. **67**, 1110 (1991).
6. E. J. Meijer, D. Frenkel, J. Chem. Phys. **100**, 6873 (1994).
7. H. N. W. Lekkerkerker, W. C.-K. Poon, P. N. Pusey, A. Stroobants, P. B. Warren, Europhys. Lett. **20**, 559 (1992).
8. T. Biben, J. P. Hansen, Phys. Rev. Lett. **66**, 2215 (1991).
9. T. Biben, J. P. Hansen, J. Phys. Condensed Matter **3**, F65 (1991).
10. J. S. van Duijneveldt, A. W. Heinen, H. N. W. Lekkerkerker, Europhys. Lett. **21**, 369 (1993).
11. J. M. Victor, J. P. Hansen, J. Physique **45**, L 307 (1985).
12. J. M. Victor, J. P. Hansen, J. Chem. Soc. Faraday Trans. 2 **81**, 43 (1985).
13. M. J. Stevens, M. O. Robbins, Europhys. Lett. **12**, 81 (1990).
14. L. Belloni, to be published.
15. D. Beysens, J. M. Petit, T. Narayanan, A. Kumar, M. L. Broide, Ber. Bunsenges. Phys. Chem. **98**, 382 (1994).
16. M. Krech, "The Casimir Effect in Critical Systems", World Scientific, Singapore, 1994.
17. For a review see: H. Löwen, Phys. Reports **237**, 249 (1994).
18. H. Löwen, T. Beier, H. Wagner, Z. Phys. B **79**, 109 (1990).
19. S. Dietrich, in: Phase Transitions and Critical Phenomena, Vol. 12, eds. C. Domb, J. Lebowitz, Academic Press, London, 1987, p.1.
20. L. J. D. Frink, F. van Swol, J. Chem. Phys. **100**, 9106 (1994).
21. P. Attard, C. P. Ursenbeck, G. N. Patey, Phys. Rev. A **45**, 7621 (1992).
22. J. P. Hansen, Phys. Rev. A **2**, 221 (1970).
23. G. Pastore, E. M. Waisman, Mol. Phys. **61**, 849 (1987).
24. R. Car, M. Parrinello, Phys. Rev. Lett. **55**, 2471 (1985).
25. H. Löwen, P. A. Madden, J. P. Hansen, Phys. Rev. Lett. **68**, 1081 (1992).
26. H. Löwen, J. P. Hansen, P. A. Madden, J. Chem. Phys. **98**, 3275 (1993).
27. M. Pearson, E. Smargiassi, P. A. Madden, J. Phys. Condens. Matter **5**, 3221 (1993).
28. H. Löwen, G. Kramposthuber, Europhys. Lett. **23**, 673 (1993).
29. J. Hoshen, R. Kopelman, Phys. Rev. B **14**, 3428 (1976).
30. D. Stauffer, Introduction to Percolation Theory, Taylor and Francis, London, 1985.
31. K. Mecke, H. Wagner, J. Stat. Phys. **64**, 843 (1991).
32. G. Gompper, M. Kraus, Phys. Rev. E **47**, 4301 (1993).
33. D. Beysens, D. Estève, Phys. Rev. Lett. **54**, 2123 (1985).
34. V. Gurfein, D. Beysens, F. Perrot, Phys. Rev. A **40**, 2543 (1989).
35. J. S. van Duijneveldt, D. Beysens, J. Chem. Phys. **94**, 5222 (1991).
36. T. Narayanan, A. Kumar, E. S. R. Gopal, D. Beysens, P. Guenoun, G. Zalczer, Phys. Rev. E **48**, 1989 (1993).
37. T. Palberg, private communication.